PROBLEMS IN ULTRA-HIGH PRECISION GPS POSITION ESTIMATION

ALEKSEI BELTUKOV, JONGHO CHOI, LEONARD HOFFNUNG,
NILIMA NIGAM, DAVID STERLING, PAUL TUPPER*

Abstract. We discuss the various techniques used to resolve integer ambiguities inherent in the measurements of GPS phase pseudoranges. In particular we formulate the problem as a mixed integer program and apply the CPLEX optimization software to simultaneously find integer ambiguities and estimate relative position. The effect of the Doppler shift is studied and a more general model for phase pseudoranges is presented. Finally, we study a two dimensional model for testing ambiguity resolution strategies, and discuss optimal satellite selection strategies. This work was conducted during the IMA Mathematical Modeling in Industry Workshop, 1998. The mentor for this project was Dr. Craig Poling, of Lockheed Martin.

Key words. Global Positioning Systems, Integer Ambiguity, Least-Squares, Doppler Shift.

1. Introduction. In the traditional commercial application of the GPS, a receiver location is determined from position and range data from some number of satellites. Typically this technique can resolve receiver positions to within tens of meters. Using local area differential GPS techniques, accuracies on the order of meters are possible [1]. Using interferometric techniques, a receiver location good to a few meters can be refined to high precision sub-centimeter location [2]. In this report we assume we have applied one of the traditional techniques to locate a receiver to within a few meters, and then we wish to apply the interferometric technique to refine the original estimate.

1.1. Goals of workshop team. Our goal is to understand the underlying mathematical problems associated with the high precision interferometric GPS techniques. The following problems were originally proposed by Dr. Craig Poling:

1. Survey methods to quickly resolve integer ambiguities, and if possible, develop a new algorithm.
2. Study a sample data set collected by Dr. Craig Poling and Brian Leininger and apply new algorithms to this data.
3. Study undesirable satellite configurations, and construct an algorithm to identify them in real time.
4. Study the potential sources of noise in this problem and if possible, enhance existing models of the problem with these corrections.
5. Construct an algorithm to identify malfunctioning satellites from observed data.

*IMA, University of Minnesota, Minneapolis. This work was conducted during the IMA Mathematical Modeling in Industry Workshop, July 22-31 1998.

Inherent in the engineering applications of GPS is the need to resolve positions quickly and accurately in real time. For the purposes of this workshop we have ignored the real-time processing constraint to gain more freedom in thinking about the underlying mathematical problems. Our approach to satisfying the workshop goals was as follows:

- Understand the mechanics of GPS interferometry, the observed physical quantities, and the basic interferometric model.
- State the problem in a mathematical form and include terms describing the contributions of noise.
- Start two concurrent efforts to generate test platforms that would provide a mechanism for testing algorithms that we developed to satisfy the stated goals :
  - Develop software to study the actual data supplied by Dr. Poling.
  - Develop a two-dimensional model and simulated data.

2. GPS Interferometry. In GPS interferometry, the observed quantity is the phase of the received cycle. Each GPS receiver generates a reference signal, and compares its phase to that of the carrier signal received from each satellite. Since phases can be measured very accurately, subcentimeter accuracies can be achieved, even though the carrier frequency considered has a wavelength of almost 20 cm[1]. Figure 1 illustrates a typical satellite receiver geometry.

With reference to this figure we have two receivers located at positions $\vec{z_A}$ and $\vec{z_B}$. In the general problem receiver A is fixed but receiver B may be moving in time. One may seek to determine the position of receiver B with respect to A (position determination), or, as described in [2] one might also consider the distance between A and B known, and wish to determine the relative orientation of receiver B (attitude determination). For this workshop, we restrict ourselves to fixed-receiver position determination. The geometry of this problem stems from our assumption that the distance between the receivers is very small when compared to the distance from each receiver to a given satellite. This is certainly the case when the receivers are separated by a few tens of meters since typical GPS satellite orbits have altitudes of almost twenty-two thousand of kilometers. Since the distance between the receivers is short in comparison to the distance to the satellites, the vectors from both receivers to a given satellite can be assumed to be parallel. A signal from satellite j arrives at receiver A earlier than at receiver B. This time lag, $\tau_B^j - \tau_A^j$, when multiplied by the speed of light, c, provides the length of the segment L. This length is the projection of the vector $\vec{z_B} - \vec{z_A}$ onto the unit vector between either receiver and the j-th satellite.

[1] See [3] for a discussion of the signal structure in current GPS applications.

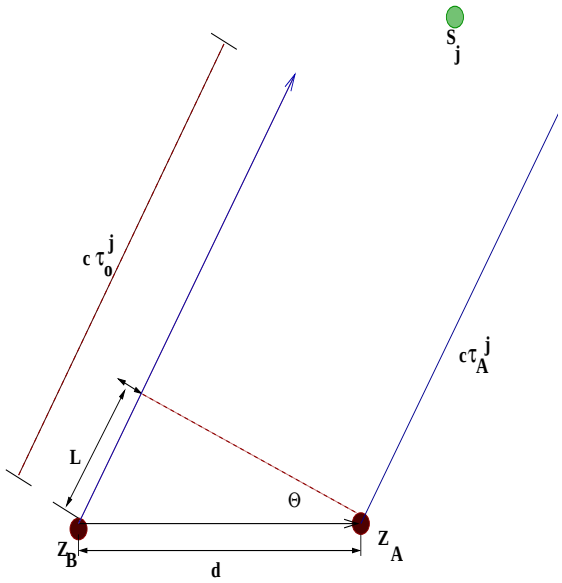

FIG. 1. *Schematic of 2-receiver, 1 satellite GPS configuration. The relative distance vector $\vec{d}$ is the quantity of interest.*

2.1. The Observables. The data used in resolving the position of the receivers consists of quantities which are directly observed, and quantities which can be derived from, the received and reference signals. These observed quantities are affected by inaccuracies in the clocks, relative motions of the satellites and the receivers, atmospheric and thermal effects, as well as other random phenomena. Techniques such as single and double differencing eliminate the effects due to clock offsets. In section 4 we seek to quantify the effects of the Doppler shift upon the observables.

The primary observed quantities are the fractional part of the beat phase $\phi^l_{A,B}(t)$, the time of transmission t_s of the signal from the satellite, the time of reception of the signal, and the angles of inclination of the satellite l with respect to the receivers A, and B. The beat phase results from the interaction of the incoming signal from the satellite and the reference signal. In this study, we concern ourselves with carrier signals on the L1 band.

3. Mathematical Model. Here we derive the mathematical model for interferometric GPS position estimation. It is convenient to adopt the notation of [3] where subscripts refer to receivers and superscripts refer to satellites. We denote a quantity $*$ from receiver A to satellite j by $*^j_A$. The difference of a quantity $*$ between receivers A and B and satellite j is denoted

$$*^j_{AB} := *^j_B - *^j_A \,,$$

and often called a *single* difference. The difference of the quantity $*$ between receivers A and B and satellites j and k is defined to be the difference between the single differences :

$$*^{jk}_{AB} := *^{k}_{AB} - *^{j}_{AB} = *^{k}_{B} - *^{k}_{A} - *^{j}_{B} + *^{j}_{A} .$$

In the following discussion $*$ will be replaced by the quantities ϕ, ψ, τ, N or n.

To construct a model of interferometric position determination we start with a receiver A and the i-th satellite. Following [2], the difference between the phase of the carrier signal sent by the i-th satellite and the reference signal generated at receiver A is given by $\psi^i_A(t)$ where

$$\psi^i_A(t) = 2\pi f_c \tau^i_A(t) + 2\pi f_c(\Delta t_A - \Delta t^i) .$$

Here, f_c is the carrier frequency, τ^i_A is the time lag from satellite i to receiver A, and $\Delta t_A, \Delta t^i$ are biases on the clocks of receiver A and satellite i respectively. When a receiver is switched on at epoch T_0, it measures the instantaneous fractional phase difference between the reference and received signals. The integer number of cycles between satellite i and receiver A is unknown. While receiver A remains locked on satellite i this integer cycle ambiguity, denoted N^i_A, remains constant. We express the phase difference $\psi^i_A(t)$ explicitly as

$$\psi^i_A(t) = \phi^i_A|^t_{T_o} + 2\pi N^i_A ,$$

where $\phi^i_A|^t_{T_o}$ is the fractional part of the phase augmented by 2π times the number of integer cycles that have elapsed since signal acquisition at T_0. In the subsequent discussion we drop the explicit reference to the initial epoch, T_0 in our notation, but ϕ^i_A is still understood to be the fractional part of the observed phase difference plus 2π times some small number of integer cycles that have elapsed since acquisition. Expressing the phase difference with ϕ^i_A we make the instantaneous integer cycle ambiguity explicit

$$\phi^i_A(t) = 2\pi f_c \tau^i_A(t) + 2\pi f_c(\Delta t_A - \Delta t^i) - 2\pi N^i_A . \tag{3.1}$$

Equation (3.1) contains two clock biases which we can we can remove by successive differences. Since the satellite clock bias, Δt^i is independent of which receiver we use, we can remove it by differencing the fractional phases from a pair of receivers. In the GPS literature this is called the *first difference* in the phase measurements from satellite i to receivers A and B

$$\begin{aligned}\phi^i_{AB}(t) &\equiv \phi^i_B(t) - \phi^i_A(t) \\ &= 2\pi f_c(\tau^i_B(t) - \tau^i_A(t)) + 2\pi f_c(\Delta t_B - \Delta t_A) - 2\pi(N^i_B - N^i_A) .\end{aligned}$$

We have removed the clock bias from satellite i, but at the expense of introducing another clock bias at receiver B. The receiver clock biases

are independent of the satellite we use so we can difference them away by introducing a second satellite. We compute the *double difference* between receivers A and B and satellites i and j as

$$\begin{aligned}\phi_{AB}^{ij}(t) &\equiv \phi_{AB}^{j}(t) - \phi_{AB}^{i}(t) \\ &= 2\pi f_c[\tau_{AB}^{j}(t) - \tau_{AB}^{i}(t)] - 2\pi N_{AB}^{ij}\end{aligned}$$

Using the satellite receiver geometry illustrated in Figure 1 the difference in time lags between receivers A and B with satellite i is given by

$$c(\tau_B^j - c\tau_A^j) = c\tau_{AB}^j = (\hat{k}^j)^T(\vec{z}_A - \vec{z}_B)\,. \tag{3.2}$$

With this relation and using $\lambda = c/f_c$ we have

$$\phi_{AB}^{ij}(t) = -\frac{2\pi}{\lambda}(\hat{k}^j(t) - \hat{k}^i(t))^T(\vec{z}_B - \vec{z}_A) - 2\pi N_{AB}^{ij}\,. \tag{3.3}$$

The quantity $\phi_A^j(t)$ contains a fractional part plus 2π times the number of cycles that have elapsed since T_0. The actual observed quantity is called the Integrated Carrier Phase (ICP) and for convenience we denote

$$ICP_A^i(t) \equiv \frac{\phi_A^i(t)}{2\pi}.$$

The ICP contains the fractional part of the phase plus some small number of integer cycles that have elapsed since acquisition. We express (3.3) in terms of ICP as

$$-\hat{k}^{ij}(t)^T\vec{z}_{AB} - \lambda N_{AB}^{ij} = \lambda ICP_{AB}^{ij}(t)\,, \tag{3.4}$$

which is a single equation in four unknowns (three components of $\vec{z}_{AB}$ and the integer N_{AB}^{ij}). We can bound the integer ambiguity N_{AB}^{ij} with

$$|N_{AB}^{ij}| \leq 2\frac{||\vec{z}_{AB}||}{\lambda} + |Integer[ICP_{AB}^{ij}(t)]| + 1 \tag{3.5}$$

This bound gives us a way of determining the range of possible ambiguities at any point in time using a rough estimate of the position and knowledge of how many integer cycles have elapsed since acquisition.

The problem of determining the relative position, $\vec{z}_{AB}$, between receivers A and B using phase measurements from M satellites is stated formally as follows:

$$\min_{\substack{x\in\mathbb{R}^3 \\ n\in\mathbb{Z}^M}} \left|\left|\mathcal{A}_K(t)x + B_\lambda n - (b(t)+\eta)\right|\right|. \tag{3.6}$$

In (3.6) we denote the measurement noise explicitly with η. The rows of $\mathcal{A}_K(t)$ are given by the first term in (3.4) while the rows in B_λ are given

by the second term. When the system is square B_λ is λ times an identity matrix. The right hand side vector, b is simply the right hand side of (3.4). The system of equations (3.6) is written out explicitly in the two dimensional model below. We reviewed several attempts [4, 5, 6] to solve (3.6) and in each case the authors chose the following basic strategy:

1. Solve (3.6) with $n \in \mathbb{R}^M$. This is called the floating point ambiguity solution.
2. Apply some sort of heuristics to force the floating point ambiguities to be integers. Often this involves statistical estimation over many epochs.
3. Resolve (3.6) with n constrained to be the integer ambiguity vector determined in the previous step.

The success of this strategy depends on the quality of the heuristics applied to sort out the integer ambiguities. In Section 6 we used a branch and bound algorithm in the CPLEX optimization package to solve (3.6).

In the following section, we seek to include the effects of the Doppler shift explicitly in the model for the beat phase, (3.1). This introduces a non-linearity in the system (3.6). However, the constraint of a short base-line is now removed.

4. The Doppler Shift as an Observable. In this section, we develop the mathematical theory for the phase pseudoranges, while retaining the Doppler effects. These Doppler effects depend on the relative velocities of the satellites and the receivers, and clearly depend upon the angle of elevation of the satellite in the receiver's sky. The Doppler shift due to a satellite located at the horizon is of the order of $4.5kHz$, whereas the carrier phase frequency is on the L1 channel, which is $1.57542GHz$. The Doppler shift has traditionally been ignored in GPS computations, on the assumption that these effects are negligible (i.e. in comparison to noise). This assumption is valid if the baselines under consideration are short, and if the tracking is not being done over too long a period of time. *This analysis was based on the work by Dr. Craig Poling in his unpublished notes.*

4.1. The Beat Phase. The phase and the associated frequency by using the relation

$$f = \frac{\partial \Phi}{\partial t}. \tag{4.1}$$

The frequency of the actual reference signal, F_A, may not be the same as desired frequency f_c. This effect can be described by

$$F_A = 2\pi[f_c + \mu_A(t + t_A)] + \delta_A(t) \tag{4.2}$$

where μ_A is the drift in the frequency generated, t is the epoch of measurement, and t_A is the receiver clock offset with respect to true GPS time. The

other random effects are included in δ_A. Therefore, the reference phase θ_A of the receiver, using relation (4.1), is

$$\begin{aligned} \theta_A(t) &= \int_{t_o}^{t} F_A(z)dz + C_A \\ &= 2\pi\left[f_c(t-t_o) + \mu_A\left(\tfrac{t^2-t_o^2}{2}\right) + \mu_A t_A(t-t_o)\right] \\ &\quad + \int_{t_o}^{t}\delta_A(t)dt + C_A \end{aligned} \tag{4.3}$$

The constant C_A is selected from physical considerations. If the receiver's clock is offset by a quantity t_A, then at time $t = t_o$ the phase is already

$$\theta_A(t_o) = 2\pi\left[f_c + \mu_A\frac{(t_o+t_A)}{2}\right](t_o+t_A) + \delta_A(t_o)\,. \tag{4.4}$$

We therefore set the constant C_A to be this initial phase. Using (4.4) and (4.3), we get, finally,

$$\theta_A(t) = 2\pi\left[f_c + \mu_A\frac{(t+t_A)}{2}\right](t+t_A) + \left(\int_{t_o}^{t}\delta_A(t)dt + \delta_A(t_o)\right). \tag{4.5}$$

The second bracket in the above expression is a noise term. We now present the integrated phase derivation for the signal from satellite j at receiver A.

The observed signal frequency, F_A^j, is not the same as the desired carrier frequency f_c. This time, the Doppler effects are carefully modeled in. If the transmitter is moving with velocity $\mathbf{V}^j(t)$, and if the receiver is moving with velocity $\mathbf{V}_A(t)$, and if the signal leaves the satellite at (true GPS) time t_1^s, and is received at (true GPS) time t_2^r, then the frequency is modeled (up to terms of order $O(\frac{1}{c^2})$) by

$$\begin{aligned} F_A^j(t) &= 2\pi\left\{f_c + \mu_j(t + t_j - \tau_A^l)\right\}\left[1 + \tfrac{\mathbf{V}^j(t_1^s) - \mathbf{V}_A(t_2^r)}{c}\cdot\hat{k}_A^j(t_1^s)\right] \\ &\quad + \delta^j(t) \end{aligned} \tag{4.6}$$

where $\hat{k}_A^j(t_1^s)$ is the unit vector between the receiver and the satellite at time t_s^1. The quantity μ_j is the amount the frequency drifts during generation, and δ^j is the noise from other sources.

Therefore, the phase $\Phi_A^j(t)$ can be obtained

$$\begin{aligned}\Phi_A^j(t) &= \int_{t_o}^t F_A^j(z)dz + C'_A \\ &= \int_{t_o}^t 2\pi \left\{ f_c + \mu_j(t + t_j - \tau_A^j) \right\} \left[1 + \frac{\mathbf{V}^j(t_1^s) - \mathbf{V}_A(t_2^r)}{c} \cdot \hat{k_A^j}(t_1^s) \right] dz \\ &\quad + \int_{t_o}^t \delta^j(z)dz + C'_A \\ &= 2\pi \left[1 + \frac{\mathbf{V}^j(t_1^s) - \mathbf{V}_A(t_2^r)}{c} \cdot \hat{k_A^j}(t_1^s) \right] \{ f_c + \\ &\quad \mu_j(\tfrac{t+t_o}{2} + t_j - \tau_A^j) \Big\} (t - t_o) \\ &\quad + \int_{t_o}^t \delta^j(z)dz + C'_A. \end{aligned} \tag{4.7}$$

Again, we choose the constant of integration, C'_A, using physical considerations. Thus, the phase of the signal received by receiver at A from satellite j is

$$\begin{aligned}\Phi_A^j(t) &= 2\pi \left(f_c + \tfrac{1}{2}\mu_j(t + t_j - \tau_A^j) \right) \beta_A^j(t_1^s, t_2^r)(t + t_j - \tau_A^j) \\ &\quad + \int_{t_o}^t \delta^j(z)dz + \delta^j(t_o) \end{aligned} \tag{4.8}$$

where the quantity

$$\beta_A^j(t_1^s, t_2^r) := \left[1 + \frac{\mathbf{V}^j(t_1^s) - \mathbf{V}_A(t_2^r)}{c} \cdot \hat{k_A^j}(t_1^s) \right]. \tag{4.9}$$

The quantity $\int_{t_o}^t \delta^j(z)dz + \delta^j(t_o)$ is the noise that is associated with the generation of the signal, as well as the noise effects that accumulate during transmission. A lot of research has been done on the causes of noise during transmission. Major factors include refractive effects introduced by the atmosphere, "multi-path effects", and errors due to the length of the receiver's antennae. Of particular interest is the atmospheric noise, which depends upon the angle the signal enters the atmosphere, the refractive index of the medium (which is layered), and the amount of time spent in each layer. A future improvement to the theory will be possible if the ionosphere, the troposphere, and low-earth atmosphere are studied in detail. For a discussion on the magnitude of the errors introduced by these effects, see , for instance, [1].

The model currently employed in interferometric GPS approximates $\beta_A^j(t_1^s, t_2^r) \approx 1$. One can actually estimate β_A^j, since satellites move at approximately $4km/s$. If we assume that $\mathbf{V}_A(t_2^r)$ is 0 at time t_r^2,

$$\|\beta_A^j(t_1^s, t_2^r)\| = \|1 + \frac{\mathbf{V}^j(t_1^s)}{c} \cdot \hat{k_A^j}(t_1^s)\| \leq 1 + \frac{4 \times 10^3}{3 \times 10^8}$$

The beat phase, $\psi_A^j(t, t_1^s, t_2^r, t)$, between the signal received at receiver A and the reference signal, is now

$$\begin{aligned}\psi_A^j(t,t_1^s,t_2^r,t) &:= -\Phi_A^j(t)+\theta_A(t)\\ &= -2\pi\left(f_c+\tfrac{1}{2}\mu_j(t+t_j-\tau_A^j\right)\beta_A^j(t_1^s,t_2^r)(t+t_j-\tau_A^j)\\ &\quad +2\pi\left[f_c+\mu_A\tfrac{(t+t_A)}{2}\right](t+t_A)\\ &\quad -\textstyle\int_{t_o}^t\delta^j(z)dz+\delta^j(t_o)+\left(\int_{t_o}^t\delta_A(t)dt-\delta_A(t_o)\right)\\ &= \phi_A^j|_{t_o}^t+2\pi N_A^j\end{aligned} \tag{4.10}$$

This beat phase depends upon the velocity of the satellite at the time the signal was generated, the velocity of the receiver at the time of receipt of this signal, the time elapsed between generation and reception, the time the beat phase is being sampled t, as well as the clock biases. The quantities $\phi_A^j|_{t_o}^t$ and N_A^i have the same meaning as in section (3).

So, suppressing the dependence on t_o,

$$\begin{aligned}\phi_A^j &= -2\pi\left(f_c+\tfrac{1}{2}\mu_j(t+t_j-\tau_A^j\right)\beta_A^j(t_1^s,t_2^r)(t+t_j-\tau_A^j)\\ &\quad +2\pi\left[f_c+\mu_A\tfrac{(t+t_A)}{2}\right](t+t_A)\\ &\quad -\textstyle\int_{t_o}^t\delta^j(z)dz-\delta^j(t_o)+\left(\int_{t_o}^t\delta_A(t)dt-\delta_A(t_o)\right)-2\pi N_A^j\end{aligned} \tag{4.11}$$

Thus, the computed double difference beat phase between satellites i, j and receivers A, B, after dropping terms of order $\mu_j\tau_{AB}^j, (\beta_A^j-1)\mu_j$ and $(\beta_A^j-1)\tau_j$, gives:

$$\begin{aligned}\phi_{AB}^{ij}(t) &= 2\pi\tau_{AB}^{ij}-2\pi N_{AB}^{ij}\\ &\quad -2\pi f_c t\beta_{AB}^{ij}-2\pi f_c(t_j\beta_{AB}^j-\beta_{AB}^i)\\ &\quad +\tfrac{2\pi f_c}{c}\left[\mathbf{V}_s^j\cdot(\hat{k}_B^j\tau_B^j-\hat{k}_A^j\tau_A^j)+\mathbf{V}_s^i\cdot(\hat{k}_B^i\tau_B^i-\hat{k}_A^i\tau_A^i)\right]\\ &\quad +\eta\end{aligned} \tag{4.12}$$

Here, η is the noise term, and is less correlated than the noise term in the usual model. We notice that the effects of the clock biases of the satellites are not completely gone. If we now linearize (4.12) about the condition $\hat{k}_A^j=\hat{k}_B^j, \hat{k}_A^i=\hat{k}_B^i$, and use the relation (3.2) we get

$$\begin{aligned}\phi_{AB}^{ij} &= -2\pi\tfrac{2\pi}{\lambda}(\hat{k}_B^j-\hat{k}_B^i)^T(\vec{z}_B-\vec{z}_A)-2\pi N_{AB}^{ij}\\ &\quad +\tfrac{2\pi f_c}{c}\left[\mathbf{V}_s^j\cdot\hat{k}_B^j\tau_{AB}^j-\mathbf{V}_s^i\cdot\hat{k}_B^i\tau_{AB}^i\right]\\ &\quad +\eta\end{aligned} \tag{4.13}$$

We notice that system (4.13) has nonlinear terms of order $\frac{f_c\mathbf{V}_s}{c}$, as compared to (3.6). With current methods, this correction is all but wiped

out by the effects of atmospheric noise. However, if extensive studies are done on the the EDC of the ionosphere, and the effects of temperature, humidity, angle of incidence and time of travel in the troposphere, the authors believe that even higher precision can be achieved, over much longer baselines than currently being used.

In addition, since the Doppler shift is a measurable quantity, using the information it contains is a useful check for damaged satellites. If the ephemeris data is incorrect, the Doppler shift can readily be used to determine a discrepancy in the velocity of the satellite.

A discussion of mixed optimization techniques for non-linear systems would be an interesting avenue to explore.

5. An Observation. Let S_1, S_2 be two satellites which are within the field of view of two stationary ground receivers R_1 and R_2. Then if the angles of elevation satisfy

$$\alpha_1^1 \neq \alpha_1^2, \qquad \alpha_2^1 \neq \alpha_2^2 \tag{5.1}$$

are not equal, the order of double-differencing can be chosen so as to render the integer ambiguity non-negative.

We show this first for the two dimensional case. We assume that the baseline is short (less than 100 km) such that $\alpha_1^i = \alpha_2^i$. Further, we choose satellites such that $\alpha_1^i, \alpha_1^j \in [0, \frac{\pi}{2}]$. That is, both receivers have the same angles of elevation to a given satellite. (see figure (2). Let N_A^j and N_B^j be the total number of wavelengths between satellite j and receivers A and B, respectively. Then,

$$\begin{aligned} \Phi_{AB}^j(t) &= (- \triangle \phi_B^j|_{t_\circ}^t - 2\pi N_B^j) - (- \triangle \phi_A^j|_{t_\circ}^t - 2\pi N_A^j) \\ &= 2\pi(N_A^j - N_B^j) + \left[\triangle\phi_A^j|_{t_\circ}^t - \triangle\phi_B^j|_{t_\circ}^t\right] \end{aligned} \tag{5.2}$$

In figure (2), the distance $\|p - Z_A\|$ can be represented in terms of cycles, and

$$\begin{aligned} \lambda_c \left|N_A^j - N_B^j\right| &= Integer\|p - Z_A\| = Integer\left(d_{AB}\cos(\alpha_A^j)\right) \\ &\quad and \\ \lambda_c \left|N_A^k - N_B^k\right| &= Integer\|q - Z_A\| = Integer\left(d_{AB}\cos(\alpha_A^k)\right). \end{aligned} \tag{5.3}$$

If both α_A^j and α_A^k are less than $\frac{\pi}{2}$, the absolute value signs in (5.3) can be dropped. Note that elevation angles lie in the range $0 \leq \alpha_A^j \leq \pi$. Thus, if $\alpha_A^j > \alpha_A^k$, subtracting the ICP data of satellite k from that of satellite j gives the second difference equation

$$\Phi_{AB}^{kj} = 2\pi\left[(N_A^j - N_B^j) - (N_A^k - N_B^k)\right] + \triangle\phi_{AB}^{kj}|_{t_\circ}^t \tag{5.4}$$

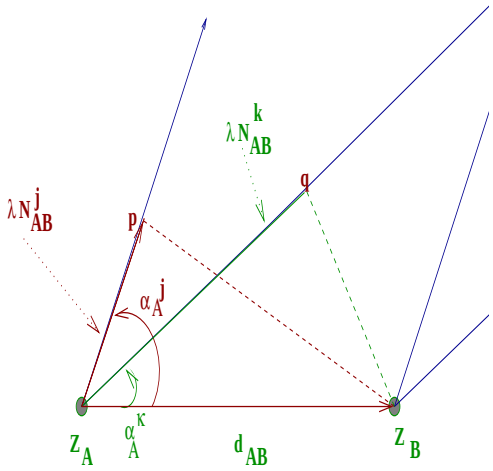

FIG. 2. *Z_A and Z_B are stationary receivers on the ground. α_A^k, α_A^j are the angles of elevation of satellites k and j, respectively. The baseline d is short.*

The quantity in the square brackets in (5.4) is negative, since $\cos(\alpha)$ is a strictly decreasing function over $[0, \frac{\pi}{2}]$.

In the three dimensional case, suppose that the angles of elevation and the azimuth angles of the two satellites, i, j with respect to the receiver A, are α_A^i, α_A^j and γ_A^i, γ_A^j, respectively. Then, the quantity $L1 = c\tau_{AB}^i = \hat{k}_A^i \cdot (\vec{z}_B - \vec{z}_A)$ and $L2 = c\tau_{AB}^j = \hat{k}_A^j \cdot (\vec{z}_B - \vec{z}_A)$.

We now project the quantity $L1$ onto the same azimuthal plane as $L2$. Denoting this projection by $L1_{new}$, we get

$$L1_{new} = L1 \cos(\gamma_A^i - \gamma_A^j).$$

Now we can use the result from the two-dimensional case, and notice that the integer ambiguity will be positive or negative depending on the sign of

$$L2\cos(\alpha_A^j) \quad -L1_{new}\cos(\alpha_A^i) = \left(\hat{k}_A^j \cos(\alpha_A^j) - \hat{k}_A^i \cos(\gamma_A^i - \gamma_A^j)\cos(\alpha_A^i)\right) \cdot (z_B - z_A) \tag{5.5}$$

The usefulness of this observation depends on the pay-off between computation time needed to find the sign of (5.5), and then build the matrix for (3.6), and the time required to search through $2N$ versus N integers for each satellite, where N is given by (3.5). For instance, if we can order the second differences to give only non-negative integer ambiguities, then we need only search for over half the integer space currently used for one

satellite, one fourth the space used for two satellites, and so forth. The authors were not able to compare these methods, and hope to do so at a later date.

6. Mixed Integer Programming. We were given three sets of ICP data to test our integer resolution strategies. The data sets contained 10 seconds, 30 minutes and 4 hours of data collected from three separate receivers (0,1, and 2). We were also given double differenced ICP data with the integer ambiguities removed so we could check our procedures against a reference solution. Our hope was to solve (3.6) using this data and some simple techniques. We expected that the simple strategies would fail and when they failed we hoped to gain some insight that would help us design a better strategy. Since (3.6) is a mixed integer program it seems natural to use techniques from the optimization community. In particular, we tried a branch and bound technique using the CPLEX[2] optimization package. CPLEX is an optimization package that will solve mixed integer programming problems (among other things). CPLEX accepts a high level description of the problem which makes it very easy to use. For example, here's a CPLEX input file to solve (3.6) for a particular pair of epochs:

```
minimize s1 + s2+ s3+ s4+ s5+ s6+ t1+ t2+ t3+ t4+ t5+ t6
st
-0.1686 x1+  0.5873 x2+  0.9129 x3  -19.0293 x4  -0.0000 x5  -0.0000 x6+ s1 -t1 = -6858340.1528
-0.7671 x1+  0.3763 x2+  0.3495 x3  -0.0000 x4  -19.0293 x5  -0.0000 x6+ s2 -t2 = -1953782.6715
 0.2470 x1  -0.6899 x2+  0.1112 x3  -0.0000 x4  -0.0000 x5  -19.0293 x6+ s3 -t3 = -17877448.2813
-0.1667 x1+  0.5856 x2+  0.9160 x3  -19.0293 x4  -0.0000 x5  -0.0000 x6+ s4 -t4 = -6858340.61527
 0.7654 x1+  0.3730 x2+  0.3474 x3  -0.0000 x4  -19.0293 x5  -0.0000 x6+ s5 -t5 = -1953782.9855
 0.2498 x1  -0.6892 x2+  0.1110 x3  -0.0000 x4  -0.0000 x5  -19.0293 x6+ s6 -t6 = -17877448.3174
Bounds
-200 <= x1 <= 200
-200 <= x2 <= 200
-200 <= x3 <= 200
-2100000 <= x4 <= 2100000
-2100000 <= x5 <= 2100000
-2100000 <= x6 <= 2100000
integers
x4
x5
x6
end
```

The values have been truncated to four decimal places for presentation and the constraints chosen are for illustration purposes. The s and t variables are the slack variables used in the formulation of the linear program. Here is a typical output listing from a CPLEX session :

```
Welcome to CPLEX Linear Optimizer 4.0.8 with Mixed Integer Solver
Copyright (c) CPLEX Optimization, Inc., 1989-1995
CPLEX is a registered trademark of CPLEX Optimization, Inc.

CPLEX> Problem name: epoch101_111.cplex
Constraints        :       6  [Equal: 6]
Variables          :      18  [Nneg: 12,  Box: 3,  Integer: 3]
Constraint nonzeros:      36
Objective  nonzeros:      12
RHS        nonzeros:       6
CPLEX> No MIP presolve or aggregator reductions.
Presolve time =    0.00 sec.

Using rounding heuristic, 2 variables fixed:
```

[2]We are grateful to Dr. Samer Takriti for his help with CPLEX

```
        Nodes                                         Cuts/
   Node  Left     Objective  IInf  Best Integer     Best Node    ItCnt

      0+    0        0.0019     1                     0.0019       11
*     1+    1        2.0282     0        2.0282       0.0019       14

Done with heuristic.
        Nodes                                         Cuts/
   Node  Left     Objective  IInf  Best Integer     Best Node    ItCnt

      0     0        0.0000     3        2.0282       0.0000       14
*     7     2        0.0539     0        0.0539       0.0083       23
*    13     0        0.0109     0        0.0109                    31

Integer optimal solution:  Objective =    1.0933117097e-02
Solution time =    0.02 sec.    Iterations = 31   Nodes = 13

CPLEX> Variable Name           Solution Value
s1                            0.005452
s3                            0.000048
t2                            0.005434
x1                         -108.082786
x2                         -175.549600
x3                          -36.440990
x4                       360402.000000
x5                       398981.000000
x6                       939471.000000
```

Here we see that CPLEX found a solution with residual error roughly 0.001 cm in 0.02 sec. The three coordinates of the relative position, $\vec{z}_{AB}$, are given in the variables $x1, x2, x3$ and the three integer ambiguities are given in $x4, x5, x6$.

As mentioned in section 3, the matrix $\mathcal{A}_k(t_1, t_2)$ can be fairly ill-conditioned if either a bad satellite geometry is chosen or the epochs t_1 and t_2 are too close together. We were able to illustrate both of these concerns using CPLEX. Figure 3 shows the mean distance computed by CPLEX over four minutes of ICP data from receiver 0 for two different satellite geometries and several different time lags.

Over this period of time the actual mean distance between receivers 0 and 1 was about 73 centimeters. Thus, even using the optimal satellites and the 20 second time lag, the CPLEX solution was more than half a meter off. At each of the CPLEX solutions the residual error was less than a centimeter so CPLEX was returning good solutions. Notice that the CPLEX solution for the good satellite geometry is significantly better than that for the average geometry.

Regrettably we did not have time to pursue the discrepancy between the CPLEX solution and the answer given by Dr. Poling. It is quite likely that (3.6) has several feasible solutions and so we should not expect that there is a *unique* solution, especially in the presence of noise (η). Just how many solution exist and how disparate they are, are two key questions that we failed to address. In the end we spent a lot of time trying to understand the data (and hence be sure that we had given CPLEX the correct problem to solve). In retrospect, we probably were interpreting the data correctly all along, but failed to recognize that the problem had multiple solutions.

In an effort to prevent having all our work hinge on our understanding/interpretation of the data set we had been given, we constructed a two dimensional model of the satellite/receiver geometry. We used this model so some of the group could study ambiguity resolution strategies while the rest struggled to understand the data we had. We discuss the

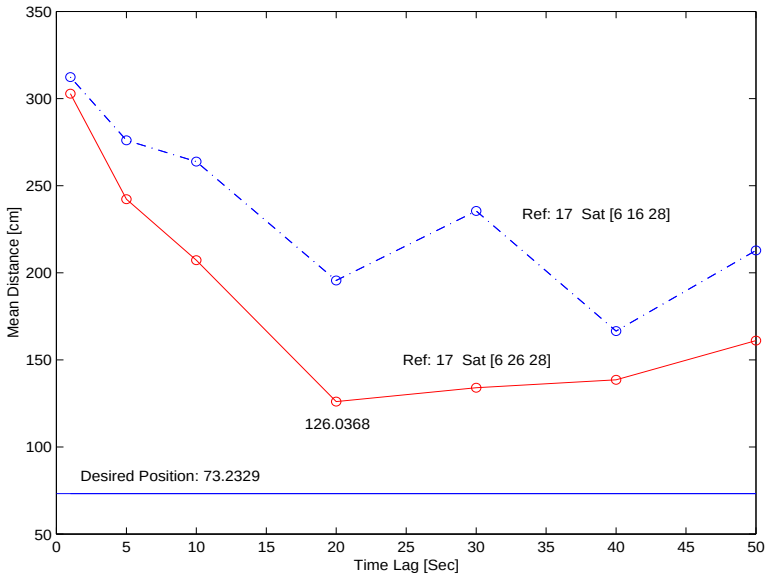

FIG. 3. *CPLEX solutions for two different satellite geometries and several different time lags between the measurement epochs*

two dimensional model in the next section.

7. A Two-dimensional Model of Ultra-high Precision GPS. As a simple tool to explore some of the features of GPS, a two-dimensional computer model was created. In the model, the earth is a disk of radius 1. Satellites are moving in a circular orbit, of radius 4, concentric with the earth. One receiver is located at the north pole of the disk, and a second receiver is displaced 10^{-4} units to the right along the tangent line to the circle. We take the position of the first receiver to be known, and we will ascertain the position of the other receiver through GPS.

Six satellites are randomly placed on the outer circle so that they are all visible to the two receivers. They move along the circle at uniform angular velocities. Three move clockwise whereas the others move counter-clockwise.

From (3.4) at epoch t_k we have,

$$-\hat{k}^{ij}(t_k)^T(\vec{z}_{AB}) - \lambda N^{ij}_{AB} = \lambda \left[ICP^{ij}_{AB}(t_k) \right] \tag{7.1}$$

Here, the difference in the unit vectors $\hat{k}^{ij}(t_k)$ is calculated exactly from the geometry of the problem (see figure(1)). The true integrated carrier phases are likewise generated from geometric considerations, and are then perturbed by randomly generated noise with the appropriate covariance structure to yield the observables $ICP^{ij}_{AB}(t_k)$.

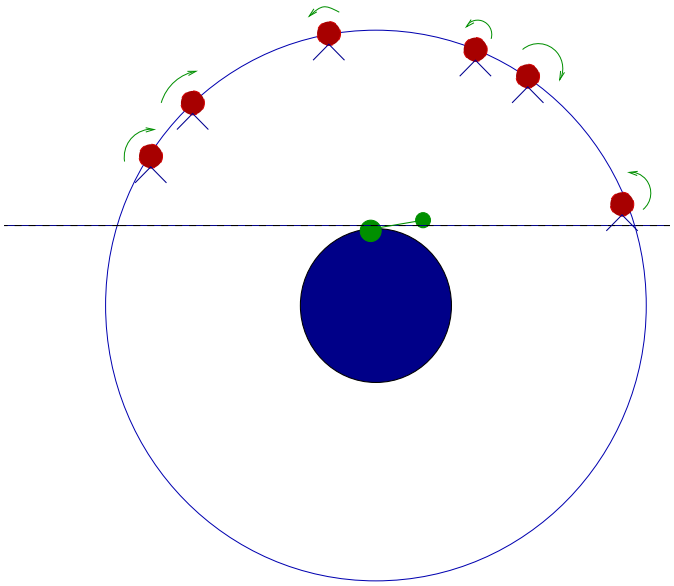

FIG. 4. *The two-dimensional model.*

Each pair i, j of satellites and each epoch considered introduces a new equation to our system. For example, suppose we have the satellites 1,2, and 3, and we sample at times t_1 and t_2. We designate satellite 1 as our reference satellite, forming two satellite pairs $\{1,2\}, \{1,3\}$. This yields the system

$$\begin{bmatrix} -\hat{k}_T^{12}(t_1) & -\lambda & 0 \\ -\hat{k}_T^{13}(t_1) & 0 & -\lambda \\ -\hat{k}_T^{12}(t_2) & -\lambda & 0 \\ -\hat{k}_T^{13}(t_2) & 0 & -\lambda \end{bmatrix} \begin{bmatrix} \vec{z}_{AB} \\ N_{AB}^{12} \\ N_{AB}^{13} \end{bmatrix} = \lambda \begin{bmatrix} ICP_{AB}^{12}(t_1) \\ ICP_{AB}^{13}(t_1) \\ ICP_{AB}^{12}(t_2) \\ ICP_{AB}^{13}(t_2) \end{bmatrix} \tag{7.2}$$

where $\hat{k}_T^{ij}(t_k)$ denotes the transpose of $\hat{k}^{ij}(t_k)$.

In this case, there are four equations in four unknowns ($\vec{z}_{AB}$ has two components) so a unique solution exists. Considering more satellites or more epochs leads to more equations than unknowns, and thus the equations can only be solved in a least-squared sense.

We considered two different methods for solving the system. Method I consists of ignoring the fact that the N_{AB}^{ij} are integer-valued, and solving the system as an ordinary least-squares problem. The $\vec{z}_{AB}$ computed in this way is taken to be our estimate of the receiver's position.

Method II extends method I with a crude method to obtain integer values for the N_{AB}^{ij}. First, method I is applied to obtain the real-valued $\vec{z}_{AB}$ and N_{AB}^{ij}. These N_{AB}^{ij} are then rounded to the nearest integer values.

They are then plugged back into the system and held fixed, as least-squares is applied to obtain a new approximation for $\vec{z}_{AB}$.

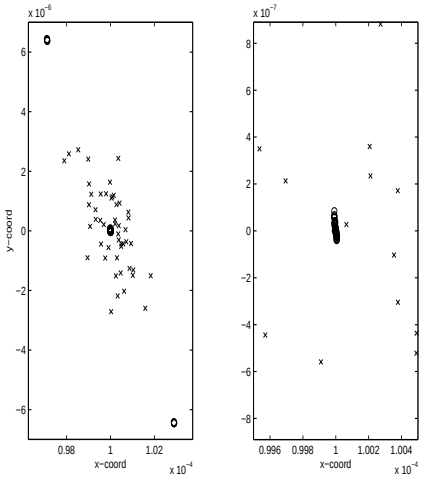

FIG. 5. *Left: A comparison of the position resolution of method I (x) and method II (o). Right: A close-up at the location of the correct solution.*

Figure (5) displays the results of these two methods when applied to data generated by the two-dimensional model. In this case, three satellites were used over two epochs. Each method was applied fifty times to the problem, each time with different random noise added to the ICP. Crosses indicate method I, and circles denote method II. The first plot shows all the data collected, and the second shows a magnification of the area around the actual solution of $x = 10^{-4}, y = 0$. Method I is seen to generate a cluster of points around the correct solution, with a mean position of $(1.00038 \times 10^{-4}, 9.8 \times 10^{-8})$ with standard deviations in x and y of $(8.08 \times 10^{-7}, 1.33 \times 10^{-6})$. Method II generates three tight clusters, the one at the correct location having forty of the fifty resolved points. The other ten points resulted from an improper resolution of the ambiguities. If we only consider data from the cluster with the correct ambiguity resolution, these points have mean position of $(9.9998 \times 10^{-5}, 7.603 \times 10^{-9})$ and standard deviation $(5.306 \times 10^{-9}, 3.14 \times 10^{-8})$, two orders of magnitude lower than the method I results. Of course, these numbers are only comparable if we use a better method of integer ambiguity resolution than the one used by method II.

One method of improving ambiguity resolution is to use data from additional satellites. An example of this technique is shown in figure (6).

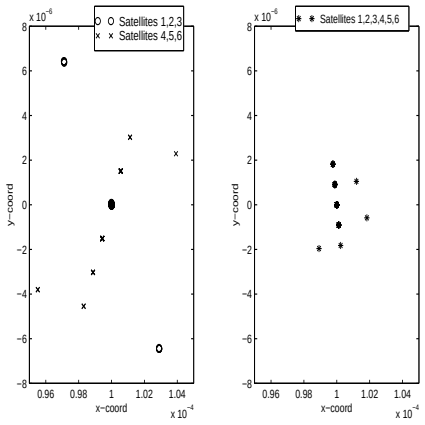

FIG. 6. *Left: Method II applied using two disjoint trios of satellites. Right: Method II applied using both trios together.*

In the first plot, method II is applied using two disjoint trios of satellites over two epochs. Fifty trials are shown. Since the spacing between clusters of data is on the order of a wavelength, if in one trial the distance between the two position estimates is small enough, we can be reasonably sure that we have resolved the ambiguities correctly. Otherwise, we must collect more data, or try other configurations of satellites.

As a comparison to this technique, the second plot of figure (6) shows the result of solving the equations for the two trios of satellites as one system using method II. The data does not lie in the correct cluster with as high probability as in the first case, and there is no way to verify if the resolution of the integer ambiguities is correct.

Any method used for the resolution of the ambiguities can be improved by starting out with a finite range of possible integer ambiguities. This can be done by obtaining a *very* rough estimate of $\vec{z}_{AB}$ using traditional GPS techniques. If we know that this result is accurate to a certain distance, say 100 meters, then we then know that the true position lies somewhere within a ball with a radius of this distance.

If we choose a trio of satellites, each pair of integer ambiguities N_{AB}^{ij}, N_{AB}^{ik} that we might choose yields a different position $\vec{z}_{AB}$. However, from our rough estimate, we need only consider those integer ambiguities which yield a $\vec{z}_{AB}$ within the ball. There are only a finite number of such pairs. From the linearity of equation (7.2), it can be seen that $\vec{z}_{AB}(N_{AB}^{ij}, N_{AB}^{ik})$

generates a uniform grid of possible locations. We want to select satellites so that the grid is widely spaced, leaving as few potential points in the ball as possible.

Bearing these considerations in mind, the two dimensional model was used to generate grids of potential points for different configurations of satellites. Two representative cases are shown in figure 7. In the first case, all three satellites are positioned relatively close together. The grid thus yielded consists of distantly spaced points. In the second case, the reference satellite and one of the others are close together, whereas the third is far away. Here, the grid distance is large in one direction, but very small in the other. These observations held for all trios of satellites; the closer the configuration of satellites, the sparser the grid, and hence the fewer the number of possible integer ambiguities.

These results can be explained by considering what happens to $\vec{z}_{AB}$ as N_{AB}^{ij} is increased by one. Denoting the projection of $\vec{z}_{AB}$ in the direction of $\hat{k}^{ij}$ as z_{AB}^{ij}, we obtain

$$\|\hat{k}^{ij}\| \left[z_{AB}^{ij}(N_{AB}^{ij}+1, N_{AB}^{ik}) - z_{AB}^{ij}(N_{AB}^{ij}, N_{AB}^{ik}) \right] = \lambda. \tag{7.3}$$

Hence the smaller $\|\hat{k}^{ij}\|$ is, the larger the change in $\vec{z}_{AB}$. i.e, the grid is spaced more widely in direction $\hat{k}^{ij}$. Since $\hat{k}^{ij}$ is the difference in the telemetry vectors between satellites i and j and the receiver A, tight satellite configuration corresponds to small $\|\hat{k}^{ij}\|$.

Another reason for using satellites that are close together is the conditioning of the matrix in equation (7.2). Suppose that satellite i is moving at a constant speed. If satellite j is close to satellite i, then the relative change of $\hat{k}^{ij}$ over one epoch will be much larger than if j is much further away. Thus, the equations for satellites i, j will be less nearly linearly dependent at the two epochs, and the matrix will be better conditioned.

7.1. The Application of Difference Matrices. In the previous section, we observed that (7.2) can only be solved in a least-squared sense when multiple sets of epoch and satellite data are used. If we have more than the minimal amount of data available, it is possible to create subsets of data, each of which give a least-squares solution. Given this set of solutions $\{z_{AB}^m, m = 1 \ldots N\}$, we can construct an $N \times N$ matrix of differences in the solutions, given by

$$D_{mn} = \|z_{AB}^m - z_{AB}^n\|.$$

Thus, each row or column n of this matrix describes the agreement between the solution z_{AB}^n and all other solutions thus obtained. Method I was applied, with difference matrices, to the two-dimensional model in Section 7.2 and a set of GPS satellite readings (described later). The

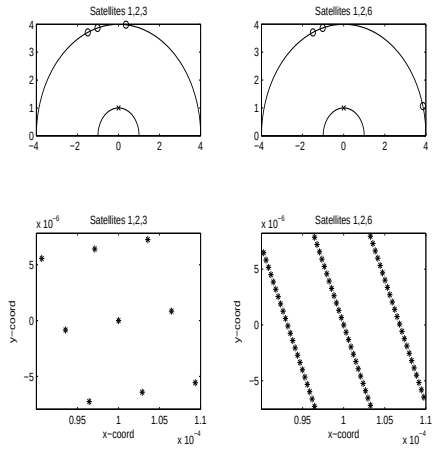

FIG. 7. *Two satellite configurations and their corresponding distributions of possible $\vec{z}_{AB}$ for different integer ambiguities.*

difference matrix D consistently possessed a small proportion of columns with disproportionately large values (see fig. (8)); we could conclude that the corresponding satellite combination is not a good approximation to the actual value of $\vec{z}_{AB}$, since its solution differs considerably from the majority of the other estimates. This behavior could result from corrupted data from the satellite, poor satellite geometry, selective availability, etc.; we will not concern ourselves with the explanation, but concentrate rather on cleaning the data by removing bad columns from D. It is interesting to observe, however, that a consistently inaccurate satellite could be deduced by the recurrence of the same bad satellite combinations over many epochs.

In the two-dimensional model, we used two types of thresholding techniques to eliminate the poor data: percentage threshold and fixed threshold. Since the model contains six satellites, there are twenty combinations of three satellites to consider. For each epoch, we solved the corresponding twenty least-squares equations, and computed D. Then, the sums of the columns were calculated and plotted. For percentage thresholding, the maximum column value was taken and all columns exceeding 80% of this value were discarded. Since a new matrix was computed during each epoch, this meant that the amount that the discarded points varied from the others differed widely from epoch to epoch; maximum column values ranged from $10 - 20$ to as high as 10^5. Therefore, the fixed threshold method was also used, where each column was discarded if it exceeded a preset amount. The

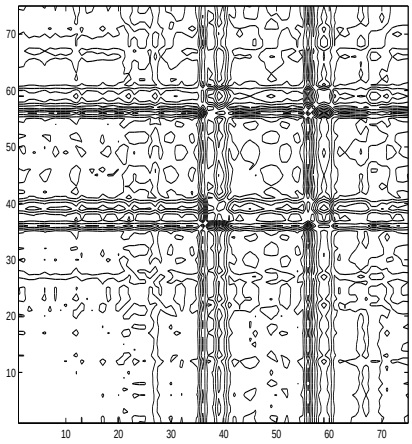

FIG. 8. *A typical Difference matrix.*

threshold was adjusted so that approximately the same number of points were discarded as in the percentage threshold, for comparison.

Both types of thresholding had similar effects; the standard deviation was reduced drastically, by as much as a factor of ten, and mean values were improved considerably. Without using difference matrix correction, the mean values were far less accurate than median; after correction, mean values improved to comparable accuracy to the median. It also appears that the median values converged much more quickly over time if corrected data was used (approximately 30 epochs were sufficient), but the accuracy was not improved significantly.

7.2. Examination of GPS Data with Method I. After studying the two-dimensional model, method I was used to find $\vec{z}_{AB}$ from actual GPS data. The data set provided contained thirty minutes of phase and ephemeris readings at one-second intervals, taken at three receivers from varying numbers of satellites. Readings at two receivers over the first thirty epochs were examined, with six satellites available. Choosing the appropriate data subsets from which to extract least-square solutions is more difficult than in the model, because the $\hat{k}_j(t)$ change only slightly between adjacent epochs. Therefore, we need to difference signals coming from significantly different epochs, else the solutions obtained vary wildly. However, requiring that the epochs be widely separated reduces the number of equations to solve and increases the statistical error in averaging those solutions. We experimentally obtained a compromise value of 5 s between

phase measurements; taking all combinations of four satellites out of six and 5 sec time differences within our 30 s file gave 825 least-square positions.

The difference matrix of all positions, compared over varying epochs, showed considerable deviation. We used a different algorithm to eliminate bad columns than those described in the previous section; instead, a more complicated algorithm was used that eliminated the largest peaks one at a time until the mean value of the column sums approached the midpoint between the minimum and the maximum. This procedure trimmed the size of the least-squares set from 825 points to 339. Plots of the column sums of D before and after the correction process are shown in figure (9); the remaining points appear to be uniformly distributed.

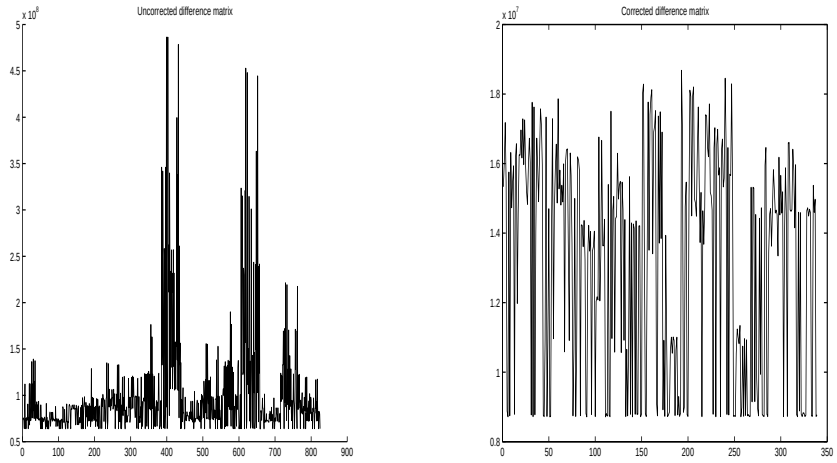

FIG. 9. *Left: The column sums before correction. Right: Column sums after correction.*

Unfortunately, the data consistency could not be improved as much as hoped. The standard deviation was reduced from 1.12 km to 305 m, which is still unsatisfactory. In all likelihood, increasing the data period from 30 seconds to several minutes or more would give much better results; this would be a logical direction to pursue in further research into this method. A subsequent test using a 30 sec data set and 10 sec between phase measurements improved the standard deviation to within 2 m. Another interesting idea would be to compare whether it is more effective to lump all points into one large difference matrix as we did here, or to evaluate a smaller matrix at each epoch as in the two-dimensional model.

7.3. The Use of Difference Matrices for Data Filtering. Let $P = (x, y, z)$ be the precise position of the receiver B with respect to receiver A, $P_i = (x_i, y_i, z_i)$ for $i = 1, ..., N$ be the different estimates of P obtained for different groups of satellites. For 20 epochs, using 8 satellites, N was 200.

If the method of solving for position is accurate than most of the points P_i will land inside a small ball $B_\epsilon(P)$. In the experiment conducted during the workshop, we used the two-dimensional model. With the radius of the Earth taken to be one unit, the dimesion of $B_\epsilon(P)$ was taken as 10^{-4} units. A point is considered "bad" if it does not lie within the confidence level. In this case, the "bad" points were those that were not inside $B_\epsilon(P)$. Few "bad" points will be scattered outside the ball $B_\epsilon(P)$ relatively far from most of the data points.

Let us assume that N_b is the number of "bad" position values and d_k is the distance from i-th "bad" point to the ball, $B_\epsilon(P)$. Let

$$X_i = \sum_{j=1}^{N} |P_i - P_j| \tag{7.4}$$

be the difference vector.

We define $X_k(bad)$ to be a vector containing the largest components of X. For "bad" points one gets an estimate on the lower bound of corresponding $X_i's$ as

$$X_k(bad) \geq (d_k - \epsilon)(N - N_b) \tag{7.5}$$

or on the average

$$\langle X_k(bad) \rangle \geq (N - N_b) * (d - \epsilon) \tag{7.6}$$

where $d =< d_k >$ whereas for "good" points one gets the following estimates

$$X_i(good) \leq \sum(d_k) + 2\epsilon(N - N_b) \tag{7.7}$$

$$\langle X_k(good) \rangle \leq N_b d + 2\epsilon(N - N_b) \tag{7.8}$$

If N is much greater than Nb and e is sufficiently small the "bad" components of the difference vector X will have much greater magnitude than the good components as shown in figure (10)

That allows one to filter out inconsistent estimates. In our method we simply removed fixed number of inconsistent values until the standard deviation of the remaining values was smaller than the threshold. This threshold was fixed empirically.

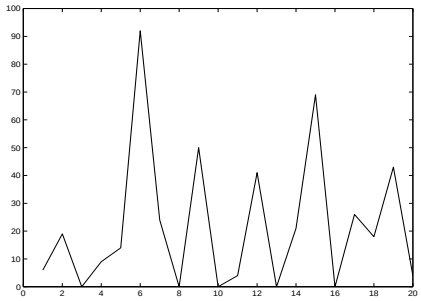

FIG. 10.

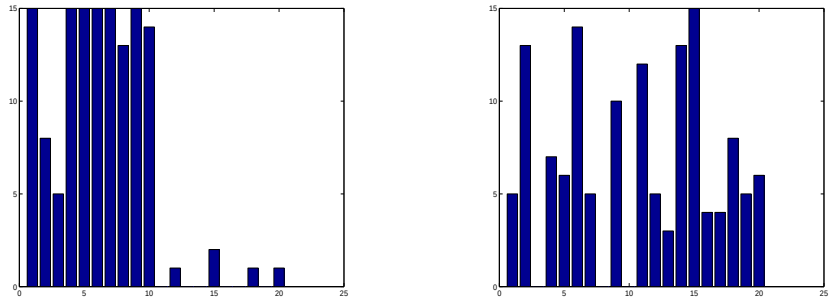

FIG. 11. *Left: Distribution with "bad" groups. Right: Distribution with "good satellites.*

Removing bad combinations of satellites does not only increase accuracy of the method but also provides a criterion for finding the damaged or "dead" satellites which constantly transmit corrupted data. If there are no damaged satellites then in the long run the odds of a patricular combination being "bad" are the same for all combinations which is not true if one or two satellites are "dead". In our experiment, the longest run consisted of 200 epochs.

We have intentionally blown up the noise level to five times the usual for particular satellites in one set of experiments and compared the distributions (see figure (11) of bad groups with that which occured normally. In almost all trials 50 epochs were enough for picking all the worst groups.

8. Satellite selection. In this section, we discuss optimal satellite selection strategies and the corresponding interferometric GPS integer am-

biguity resolution. The geometry of the visible satellites is an important factor in achieving results with high accuracy especially for relative positioning by interferometric GPS in this study. A measure for this geometry is the (relative) Dilution of Precision (DOP).

Here we consider the problem described in section 3 with two receivers A and B, two epochs, t_1 and t_2, for four satellites i, j, k, l, where i is the reference satellite for the double differences. The double differenced interferometric GPS model can be represented in a matrix-vector notation as

$$\mathbf{Ax} = \mathbf{b} \tag{8.1}$$

where

$$\mathbf{A} = \begin{bmatrix} -\hat{k}^{ij}(t_1) & -\lambda & 0 & 0 \\ -\hat{k}^{ik}(t_1) & 0 & -\lambda & 0 \\ -\hat{k}^{il}(t_1) & 0 & 0 & -\lambda \\ -\hat{k}^{ij}(t_2) & -\lambda & 0 & 0 \\ -\hat{k}^{ik}(t_2) & 0 & -\lambda & 0 \\ -\hat{k}^{il}(t_2) & 0 & 0 & -\lambda \end{bmatrix}, \tag{8.2}$$

and

$$\mathbf{x} = \begin{bmatrix} (z_{AB})_1 \\ (z_{AB})_2 \\ (z_{AB})_3 \\ N_{AB}^{ij} \\ N_{AB}^{ik} \\ N_{AB}^{il} \end{bmatrix}, \qquad \mathbf{b} = \lambda \begin{bmatrix} ICP_{AB}^{ij}(t_1) \\ ICP_{AB}^{ik}(t_1) \\ ICP_{AB}^{il}(t_1) \\ ICP_{AB}^{ij}(t_2) \\ ICP_{AB}^{ik}(t_2) \\ ICP_{AB}^{il}(t_2) \end{bmatrix} \tag{8.3}$$

The solution fails if the design matrix A is singular. So, the relative position between satellites is a determining factor in solving (8.1) for accurate position estimation. Good satellite geometry can be visualized as geometric diversity among the chosen satellites which results in larger determinant of A. Thus, low DOP values should reflect good satellite geometries.

In general, DOP can be calculated from the inverse of the normal equation matrix of the solution. the cofactor matrix follows from

$$\mathbf{Q_x} := \left(\mathbf{A^T P A}\right)^{-1}, \tag{8.4}$$

where $\mathbf{P}$ is the weight matrix due to the correlation from double differencing. $\mathbf{P}$ in this case is

$$\mathbf{P} = \frac{1}{8\sigma^2} \begin{bmatrix} \begin{pmatrix} 3 & -1 & -1 \\ -1 & 3 & -1 \\ -1 & -1 & 3 \end{pmatrix} & \begin{pmatrix} 0 & 0 & 0 \\ 0 & 0 & 0 \\ 0 & 0 & 0 \end{pmatrix} \\ \begin{pmatrix} 0 & 0 & 0 \\ 0 & 0 & 0 \\ 0 & 0 & 0 \end{pmatrix} & \begin{pmatrix} 3 & -1 & -1 \\ -1 & 3 & -1 \\ -1 & -1 & 3 \end{pmatrix} \end{bmatrix} \tag{8.5}$$

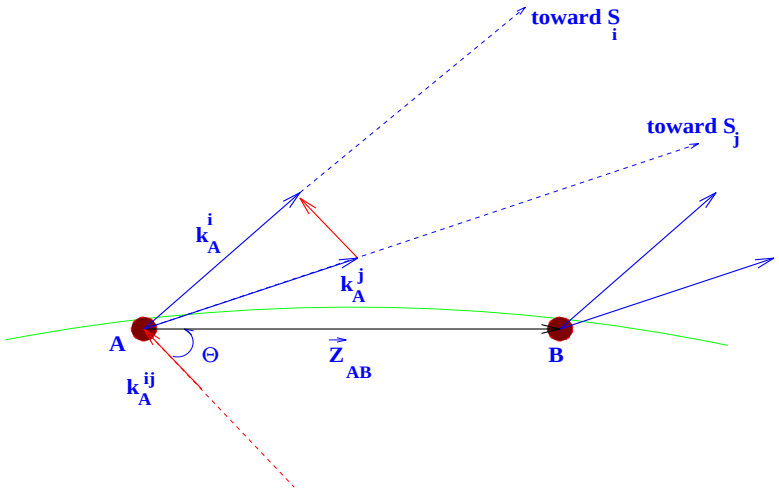

FIG. 12.

where σ^2 is the variance of ICP noise.

The Geometric Dilution of Precision (GDOP) can be used as a measure of good satellite geometry, which is defined by

$$GDOP = \sqrt{trace(\mathbf{Q_x})} \tag{8.6}$$

The condition number could also be considered as a measure of satellite geometry for a simple comparison. For a desired period, the sets of satellites with lowest GDOP and condition number can be obtained and used in initialization. In the experiments in (6), the set of satellites with best geometry was chosen over the given time periods and consistently produced superior results to those of other set of satellites. On the other hand, low DOP factor results in large number of initial ambiguity candidates. Many observation epochs and computer operations are required to resolve the correct ambiguities. Figure (12) illustrates the relation between satellite geometry and size of ambiguity candidates, since we have

$$|\bar{N}_{AB}^{ij}| \leq \frac{2|z_{AB}||\cos\theta|}{\lambda} + 1 \tag{8.7}$$

from equation (3.4).

Thus good satellite geometry has an opposite influence on the duration of the test and on error probability of the solution. Hence two different selection strategies could be proposed. First one can look for the primary set of satellites with an ideal mean value of DOP and corresponding set of the candidate primary ambiguities [6]. On the other hand, one can choose the primary satellites with best geometry to get most accurate estimate of baseline from equation (8.1), and substitute it in the equation based on

other satellite selections to find ambiguity candidates. Then least square error of each candidate is tracked down along time while ambiguity candidates exhibiting growth are ejected to narrow down the search space. Eventually the candidate that is most stable in terms of error growth will be chosen as the correct ambiguity. The former is a suitable strategy for real-time ambiguity search with less computational cost, while the latter is considered to be a good strategy for resolving ambiguity of fixed baseline.

REFERENCES

[1] B. Parkinson and Enge P. Differential gps. *Global Positioning System: Theory and Applications*, 2, 1995.

[2] Friedman A. *Mathematics in Industrial Problems*, volume IMA Volume 88. Springer-Verlag New York, 1997.

[3] Lichtenegger H. Hofmann-Wellenhof, B. and Collins J. *GPS, Theory and practice. Third Edition.* Springer-Verlag New York, 1992.

[4] Teunissen P.J.G. A new method for fast carrier phase ambiguity estimation. *Conference Proceeding Communicated by Dr. Poling*, pages 562–573, 1994.

[5] Masson A. Burtin D. and Sebe M. Kinematics dgps and ins hybridization for precise trajectory determination. *Conference Proceeding Communicated by Dr. Poling*, pages 299–308, 1995.

[6] C. Macabiau. A new concept for gps phase ambiguity resolution on-the-fly: The maximum a posteriori ambiguity search(mapas) method. *Proceedings of ION GPS-95, the Institute of Navigation*, pages 299–308, 1995.